Appl. Phys. A 81, 1221–1226 (2005)
DOI: 10.1007/s00339-005-3306-1

Applied Physics A
Materials Science & Processing

L. ESCOBAR-ALARCÓN[1,✉]
E. CAMPS[1]
M.A. CASTRO[1]
S. MUHL[2]
J.A. MEJIA-HERNANDEZ[1,2]

Effect of the plasma parameters on the properties of titanium nitride thin films grown by laser ablation

[1] Departamento de Física, Instituto Nacional de Investigaciones Nucleares, Apartado Postal 18-1027, México DF 11801, México
[2] Instituto de Investigaciones en Materiales, Universidad Nacional Autónoma de México, Apartado Postal 364, México DF 01000, México

Received: 8 May 2005/Accepted: 17 May 2005
Published online: 28 June 2005 •

ABSTRACT Titanium nitride thin films were deposited at low temperatures (less than 250 °C) using the laser ablation technique. The effect of both the laser beam energy density and the gas pressure on the plasma parameters was studied. The film structure, mechanical properties and surface morphology were investigated as a function of the plasma parameters. The results showed a strong dependence of these properties on the ion kinetic energy and plasma density. The gas pressure was seen to control the preferred orientation of the films in the (200) and (111) directions. At 1×10^{-2} Torr only the (200) direction was observed. In addition, the crystal size for all the films was found to depend on the plasma parameters; generally, an increase of ion energy and plasma density resulted in a decrease of the crystal size. TiN films with hardness as high as 24.0 GPa, which is suitable for many mechanical applications, were obtained. The hardness was strongly affected by the ion energy, increasing as the ion energy increased. These results show that the properties of the deposited material are controlled in part by the degree of ion bombardment and the plasma density.

PACS 81.15.Fg; 81.05.Je; 68.55.Jk; 52.70.Ds

1 Introduction

Materials in thin-film form have received great attention partly because of their singular properties, which may differ significantly from their bulk attributes making them attractive for a wide variety of applications either as structural coatings or as functional thin films. In particular, titanium nitride (TiN) thin films have attracted the attention of many research groups because of their applications in a great variety of technological fields mainly, including mechanical applications that take advantage of the high mechanical hardness, wear and corrosion resistance of this material [1]. Specifically, in order to improve the performance and extend the life of cutting tools, a TiN film is usually used as a protective coating for stainless steel surfaces because of its high corrosion and oxidation resistance. Owing to its peculiar properties titanium nitride is also widely employed in semiconductor manufacturing as a diffusion barrier [2], as an antireflection and antistatic coating for displays [3], as a wavelength-selective transparent film [4] and also for decorative applications [5].

TiN thin films have been prepared by a variety of techniques such as magnetron sputtering, often from a titanium metal target in a nitrogen–argon atmosphere [6], by reactive evaporation [7], ion-beam deposition [8], a plasma focus device [9] and laser ablation [10, 11]. Laser ablation has been extensively used in the last few years to produce a wide variety of materials in thin-film form because of its advantages over other deposition techniques. Particularly, there are two major advantages that make this technique suitable for thin-film deposition of crystalline titanium nitride. First, the high energy of the species present in the plasma plume enhances surface mobility and thereby permits crystalline film growth at lower substrate temperatures [12, 13]; second, this technique offers the possibility for deposition in a reactive gaseous atmosphere even at high pressures [14]. The laser ablation deposition technique has been used for the preparation of a variety of hard coatings such as diamond-like carbon (DLC), c-BN and CN_x. DLC thin films have been prepared using a 248-nm excimer laser wavelength and up to 45-J/cm^2 laser energy fluence [15], or using an Nd-YAG laser with $\lambda = 1064$ nm and fluences in the range of 1–10 J/cm^2 [16]. Amorphous carbon nitride (CN_x) thin films have been deposited by pulsed laser ablation (PLA) using the infrared wavelength (1064 nm) of a Nd:YAG laser with laser fluences up to 10 J/cm^2 [17]; this material has been also synthesized using an ArF excimer laser at energy densities between 4 and 16 J/cm^2 [18]. Cubic boron nitride films have been prepared by ion-assisted pulsed laser deposition using a high laser fluence of more than 30 J/cm^2 [19].

Pulsed laser deposition (PLD) of titanium nitride (TiN) thin films has been carried out with a Nd:YAG laser (1064-nm wavelength) to ablate titanium targets in low-pressure N_2 atmospheres at room temperature and fcc stoichiometric TiN in a (111) orientation was obtained on AISI 630 HT steel and AISI M2 high speed steel substrates [20]. A frequency-doubled Nd:YAG laser (532 nm) was used to evaporate titanium targets at a fluence value of 8 J/cm^2 and at substrate temperatures from room temperature to 725 °C; the deposit obtained was of polycrystalline fcc TiN [21].

In spite of the fact that PLD has become a well-established technique for thin-film deposition, the processes involved are not well understood, and plasma characterization is a way to

✉ Fax: +52-55-53297332, E-mail: lea@nuclear.inin.mx

gain insight in determining the role of the plasma parameters on the properties of the deposited films. Particularly, the interaction of a carbon plasma in a nitrogen background gas has been investigated using laser fluences of 94 J/cm^2 of 1064-nm radiation in order to elucidate the mechanisms of formation of nitrides in the gaseous phase [22]. The formation of reactive species resulting from the plasma interaction with the N_2 atmosphere after irradiation of a titanium target with a 308-nm laser fluence of 10 J/cm^2 has been studied in order to help understand the reactive deposition process of TiN films [23].

It is worth mentioning that with the PLD technique, the thin-film properties can be varied by using an appropriate selection of the deposition parameters such as fluence, working pressure and target to substrate distance. In this way it is possible to grow materials with specific properties for tailored applications.

2 Experimental

2.1 *Experimental setup*

The laser ablation system used in this work consisted of a vacuum chamber evacuated by a diffusion pump to a base pressure of 7×10^{-6} Torr. The energy density of the Nd:YAG laser (1064 nm, 28-ns pulse duration) was varied from 7 J/cm^2 to 19 J/cm^2 by keeping the spot size constant on the target surface and adjusting the energy per pulse. The laser beam was focused with a 25-cm focal length spherical lens with an incidence angle of 45° to the target. The deposition chamber was initially evacuated to the base pressure and backfilled with a mixture, 40/60 (N_2/Ar), up to the working pressures, 5×10^{-3} Torr and 1×10^{-2} Torr. All the experiments were performed using a repetition rate of 20 Hz.

The substrates used in this study were mirror polished 4140 steel disks, 2.0-cm diameter and 0.3-cm thickness. Prior to the deposition process the substrates were ultrasonically cleaned in acetone and ethanol. The target and substrate were placed parallel and the distance between them was fixed at 3.0 cm. A resistive heater in the substrate holder was used to heat the substrate to the deposition temperature. This temperature was measured with a thermocouple mounted directly on the substrate. All the films were grown at a substrate temperature close to 230 °C. The target was rotated to avoid depletion of material at any given spot.

2.2 *Plasma characterization*

Optical emission spectroscopy (OES) was performed using a 0.5-m spectrometer (Spectra Pro 500i) equipped with a fast intensified charge-coupled device (ICCD) (Princeton Instruments model 1024E) with a 150-ns gate for photon detection. The light was collected by a UV-Vis fiber bundle placed at a side window of the vacuum chamber approximately 25 cm from the plasma. Synchronization between the laser pulse and the ICCD was ensured using a fast detector. The OES measurements were performed along the axis of the plasma, at different distances from the target surface.

Determination of the plasma parameters, the mean kinetic energy of ions and the plasma density, was performed by the time of flight technique (TOF) using a 3-mm-diameter Langmuir planar probe. In all the experiments the probe was biased at −40 V, where saturation of the ion current takes place. The signal from the probe was monitored through a 15-Ω resistor. The plasma density was determined from the ion current values across the resistor. Measurements were performed under the experimental conditions used for thin-film deposition to establish a correlation between plasma parameters and thin-film properties: that is at a distance of 3 cm from the target.

2.3 *Thin-film characterization*

The crystalline structure of the deposited films was studied by X-ray diffraction (XRD) using a Siemens D-5000 diffractometer with a Cu K_α radiation source (λ_k = 1.5406 Å). The surface morphology and the cross section of the films were observed with a scanning electron microscope (SEM, Philips XL30). The film thickness was determined with a profilometer (Sloan Dektak II). Micro-hardness measurements were performed using a Vickers micro-indenter (Shimadzu 341-64278). The surface roughness was determined using an atomic force microscope (Digital Instruments Nanoscope IV).

3 Results

Two groups of samples were prepared in the present experiments; the first was to determine the optimal growing conditions and the second to test the reproducibility of the results. In this way it was possible to study the influence of the two deposition parameters on the plasma characteristics and on the thin-film properties: the energy density used to ablate the target and the gas pressure used during deposition. In general, the deposited films show a mirror-like appearance and exhibit a golden-yellow color characteristic of TiN.

3.1 *Plasma diagnostics*

The optical emission spectroscopy results revealed a very rich emitting plasma plume due to the presence of Ti, Ti^+ and Ti^{++} excited species. It is worth noting that under the experimental conditions used in this work the most abundant species was Ti^+ and no signal associated with N or TiN was detected by OES. These results do not mean that these species are not present in the plasma and could be interpreted in terms of a nitrogen density much lower than that of the titanium species. The existence of excited neutral and ionized nitrogen species when a titanium target is ablated in the presence of a nitrogen atmosphere has been reported elsewhere but under different experimental conditions to the present work [23].

Figure 1 shows a typical set of time of flight (TOF) curves obtained from the Langmuir-probe measurements at different laser fluences for a working pressure of 1×10^{-2} Torr. It can be observed that as the laser fluence decreases the maximum in the TOF curve is shifted to longer times, indicative of a reduction of the ion kinetic energy. From these spectra the mean kinetic energy of the Ti^+ ions was obtained [24]. Figure 2 shows the mean ion kinetic energy as a function of the laser fluence for the two values of the working pressure. The ion energy shows the same tendency to increase as the laser fluence increases for each value of pressure. For the highest fluence (19 J/cm^2) and the lowest pressure (5×10^{-3} Torr) the highest

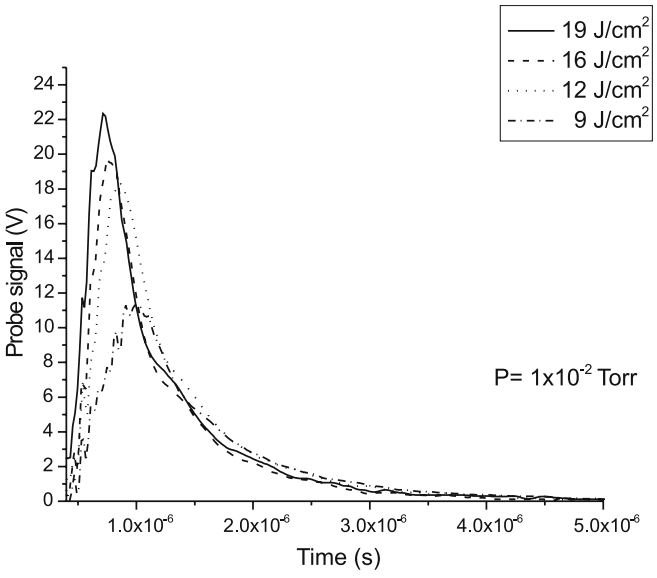

FIGURE 1 Typical time of flight (TOF) curves obtained from the Langmuir-probe measurements at different laser fluences for a working pressure of 1×10^{-2} Torr

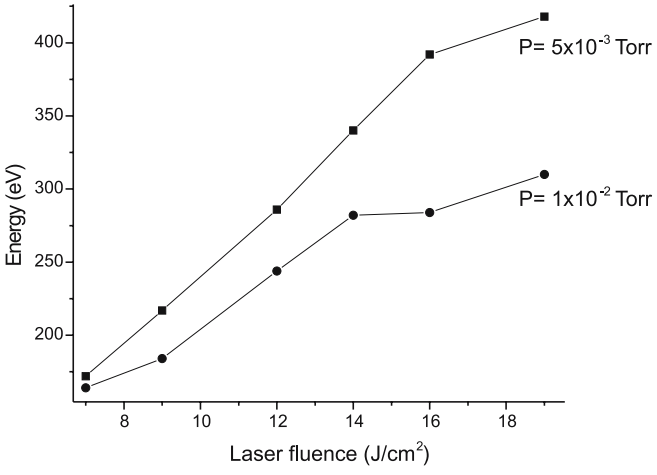

FIGURE 2 The mean ion kinetic energy of Ti II as a function of the laser fluence for two values of the working pressure

ion energy of approximately 410 eV was obtained. The lowest value of ion energy, of about 120 eV, was obtained for the lowest fluence (7 J/cm^2) and the highest pressure (1×10^{-2} Torr). The observed reduction of the kinetic energy of the plasma species as the working pressure increases can be attributed to momentum-transfer collisions between the plasma species and the background gas as the mean free path is reduced, producing a greater thermalization of the plasma plume.

The plasma density values were obtained from the mean current values calculated from the TOF curves. Figure 3 shows the plasma density as a function of the laser fluence for different values of the working pressure. It can be seen from this plot that higher laser fluence in general resulted in a higher plasma density for each pressure used. The obtained values for the plasma density fluctuate from 9.9×10^{13} cm^{-3} at 1×10^{-2} Torr and 7 J/cm^2, to 2.0×10^{15} cm^{-3} at 5×10^{-3} Torr and 19 J/cm^2. From the same figure, it is evident that the plasma density also depends on the working pressure; the density decreases as the pressure

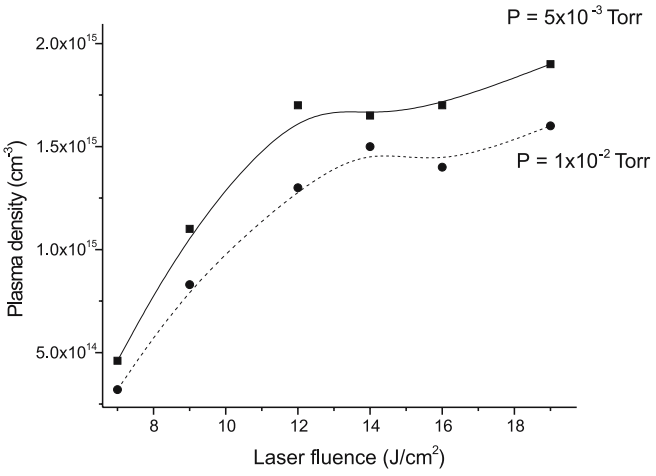

FIGURE 3 The plasma density as a function of the laser fluence for 5×10^{-3} Torr and 5×10^{-2} Torr

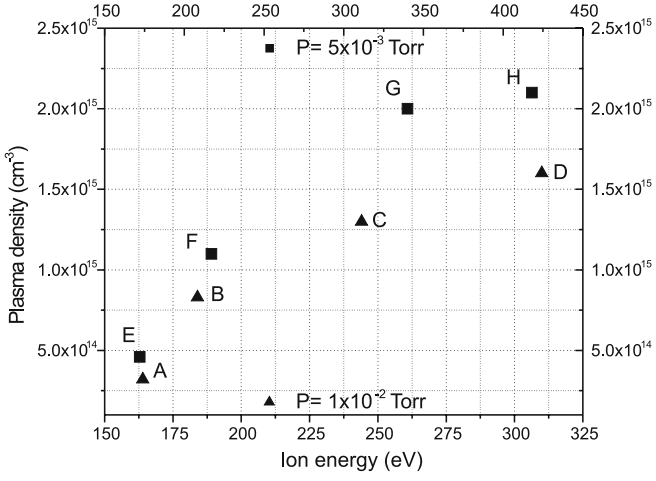

FIGURE 4 The plasma density–ion energy diagram obtained combining Figs. 2 and 3

is increased at a given laser fluence value. This behavior can be attributed to recombination processes that become more important at higher pressures as the mean free path is reduced and because the plasma beam attenuates due to multiple dispersion processes as the number of collision centers increases. At the same time, at higher pressures the plasma is confined to a smaller space and therefore fewer particles reach the probe.

By comparing the integrated ion current per pulse with the measured deposition rate (assuming single ionized atoms of Ti and the bulk density of TiN for the film) we estimate that approximately 10% of the depositing species are ionized. In spite of the fact that we are characterizing approximately only 10% of the plasma species, the studied properties of the deposited material and the variation of these with the experimental conditions can be described in terms of plasma density and mean ion kinetic energy.

From the results obtained above and combining Figs. 2 and 3, a plasma density–ion energy diagram was obtained. This diagram, shown in Fig. 4, was used to determine the plasma conditions under which deposition of films was to be carried out. For example, point A, in Fig. 4, means that the sample labeled as A was deposited using a mean ion ki-

netic energy close to 450 eV and a plasma density equal to 9.5×10^{13} cm^{-3}, and so on.

3.2 *Thin-film characterization*

3.2.1 Structural characterization. Figure 5 shows the XRD spectra of two samples (both of thickness greater than 800 nm); the first was grown using an ion energy of 184 eV and a plasma density of 8.3×10^{14} cm^{-3} (sample B in Fig. 4) and the second was grown using an ion energy of 217 eV and a plasma density of 1.1×10^{15} cm^{-3} (sample F in Fig. 4). That is, these samples were deposited at the same fluence value of 9.0 J/cm^2 but at two different working pressures, 1×10^{-2} Torr and 5×10^{-3} Torr, respectively. The spectrum corresponding to the sample deposited at 1×10^{-2} Torr is characterized by the presence of peaks at $2\theta = 42.70°$ and 93.45°, which correspond respectively to the (200) and (400) planes of cubic TiN. The fact that only these peaks are present suggests that the film has grown preferentially in the direction of the (200) plane. The additional peaks in the spectrum at $2\theta = 44.48°$, 64.78°, 82.13° and 98.5° correspond to the substrate. On the other hand, the spectrum corresponding to the sample deposited at 5×10^{-3} Torr is characterized by peaks centered at $2\theta = 36.53°$ and 77.80°, which can be attributed to the (111) and (222) planes of TiN. In this case the film has grown preferentially in the direction of the (111) plane. It is worth noting that all the samples deposited at each pressure, but at different plasma energy and density, show diffraction patterns similar to those shown in Fig. 5. These results suggest that regardless of the plasma parameters used for deposition, the working pressure plays an important role in controlling the crystalline orientation. Further work is underway in order to explain the effects of the working pressure on the plasma characteristics that result in the observed behavior.

In order to study the effect of the plasma parameters on the structural properties of the thin films, several deposits were performed at two pressures and different fluences following Fig. 4. Figure 6a presents the X-ray diffraction patterns, normalized to the thickness for comparison purposes,

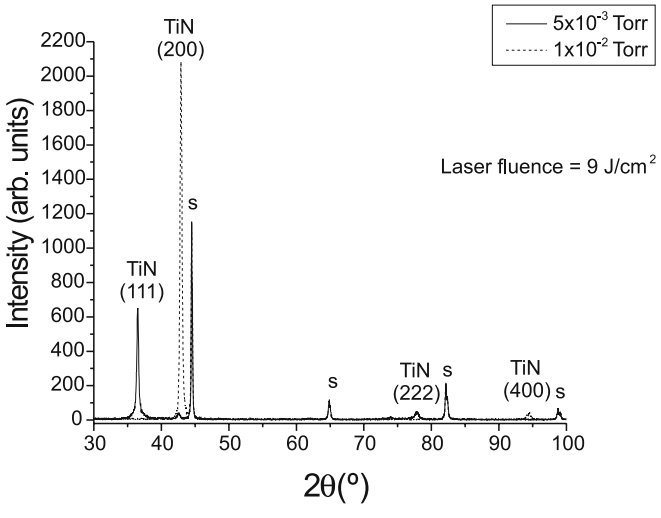

FIGURE 5 The XRD spectra of two samples grown using a fluence value of 9.0 J/cm^2 at two different working pressures, 1×10^{-2} Torr and 5×10^{-3} Torr

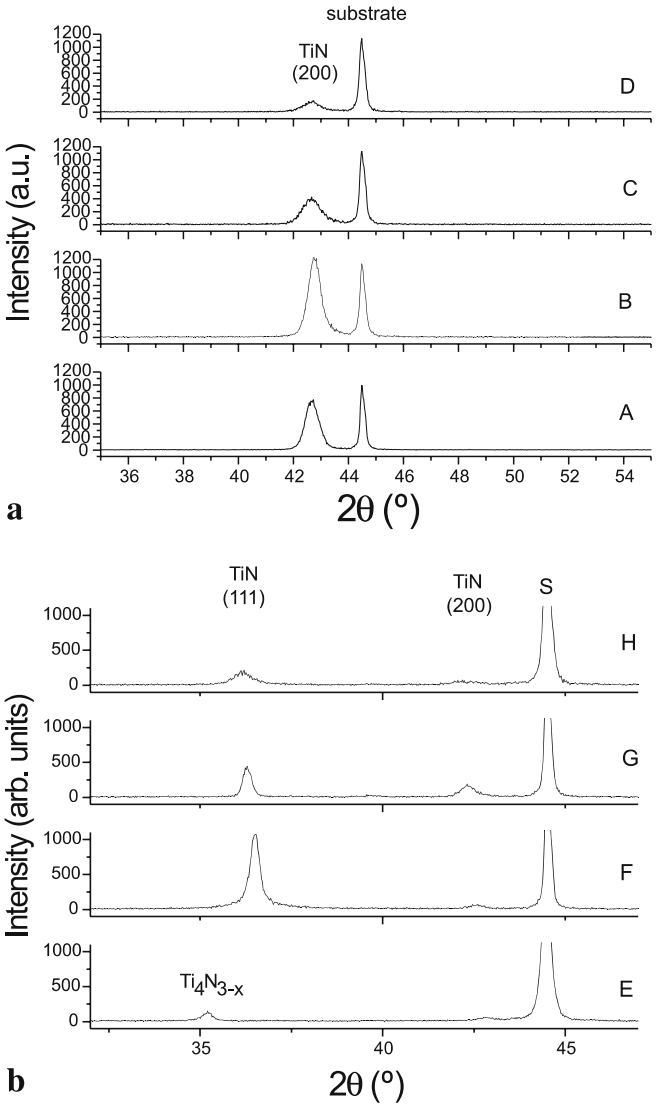

FIGURE 6 The X-ray diffraction patterns of samples deposited under different plasma conditions for 1×10^{-2} Torr (**a**) and 5×10^{-3} Torr (**b**)

corresponding to the samples labeled as A, B, C and D. At this pressure, as the ion energy increases and simultaneously the plasma density increases, the degree of crystalline quality improves first and then for ion energies greater than 184 eV the degree of crystalline quality of the film diminishes; this can be attributed to the fact that for the higher ion energies the more intense bombardment of the growing films produces an amorphization effect due to the formation of smaller crystallites.

When the pressure is set at 5×10^{-3} Torr, Fig. 6b, as was pointed before the films grew preferentially in the (111) direction with this plane parallel to the surface of the substrate. However, in this case the peak at 42.70° was still observable in the diffraction patterns but with lesser intensity. This means that at this pressure the deposited material was formed of coexisting (200) and (111) orientations. It is evident from the diffraction patterns that the (111) direction was the predominant one in these samples; in fact, the extent of the (111) orientation can be quantified by a texture coefficient defined by $I(111)/(I(111) + I(200))$ [25], where $I(h, k, l)$ is the integrated intensity of the corresponding Bragg peak. The tex-

ture coefficient for the film labeled as F was 0.94; this value indicates a high degree of orientation of this sample in the (111) direction. On the other hand, the sample labeled as H had a texture coefficient of 0.68, which was the lowest observed and means that in this sample approximately 68% of the crystalline phase was oriented in the (111) direction. It is interesting to observe that the X-ray diffraction pattern corresponding to the sample E revealed that under the deposition conditions used the deposited material was a titanium nitride deficient in nitrogen. This could be due to the fact that at this pressure there is not enough active nitrogen species to react with the titanium to produce the correct composition.

The average crystallite size as a function of the plasma parameters was estimated using the Scherrer equation, $D = 0.9\lambda/\beta \cos\theta$ [26]. The obtained results are presented in Fig. 7 where it is clear that the crystallite size is almost constant, having a value of approximately 20.5 nm for the range of ion energies from 170 to 250 eV. If higher energies are used for deposition, the grain size diminished to values close to 15 nm at 320 eV. A similar behavior was observed for the plasma density, as is also shown in Fig. 7.

3.2.2 Hardness measurements. The hardness of the TiN films was measured using a micro-indenter. Considering the indentation size effect, the load of the indenter was chosen to limit the penetration depth in order to minimize the effect of substrate on hardness of the thin film. Therefore, the hardness measurements were performed applying a 5-gf load. Given the size of the indents these were observed in the SEM in order to measure the diagonals from which an average was taken. It is well known that to obtain the hardness value for a thin film without the influence of the underlying substrate it is necessary to satisfy the requirement that the film thickness should be typically seven to ten times greater than the penetration depth. This condition is not fulfilled in our case and therefore the hardness values were determined considering a composite hardness due to the substrate contribution [27].

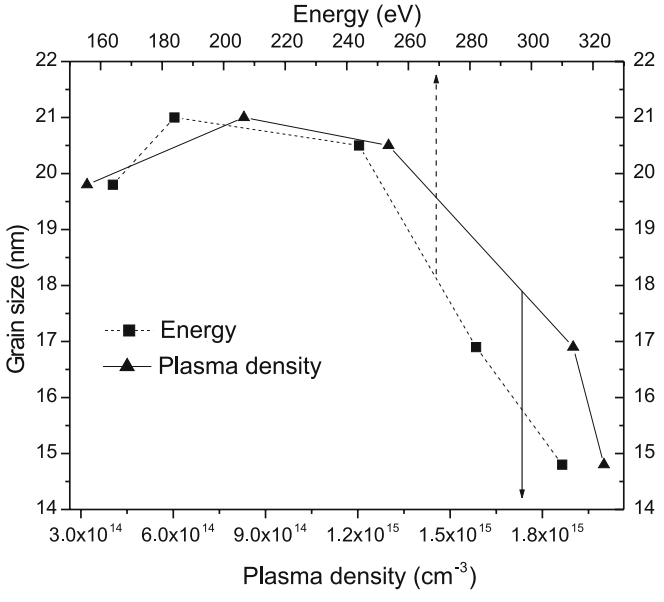

FIGURE 7 The average crystallite size as a function of the plasma parameters, ion energy and plasma density

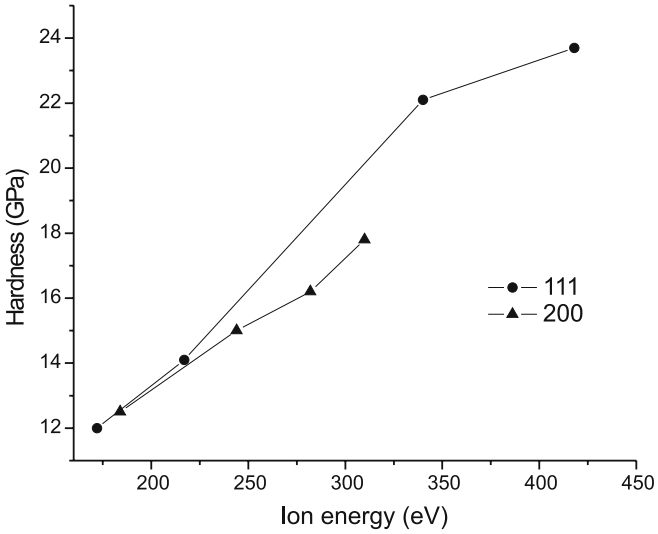

FIGURE 8 The hardness values for the films with (200) and (111) orientations as a function of the ion energy

The results show that the deposited films have hardnesses between 12 GPa and 24 GPa depending on the plasma conditions used for thin-film deposition. In Fig. 8 the hardness values for the films with (200) and (111) orientations as a function of the ion energy are presented. It can be clearly observed that the (111)-oriented films are harder than those with the (200) orientation. This result is consistent with previous reports that attribute the response to the relationship between the (111) orientation and the resolved shear stress on the slip systems of TiN [28]. Figure 8 shows that the film hardness tends to increase as the ion energy was increased; this result is consistent with the results presented in Fig. 7 since a higher hardness corresponds to a smaller grain size.

3.2.3 Morphology. The scanning electron microscopy images of the deposited thin films showed smooth surfaces with a small number of scattered particles, as shown in Fig. 9a; the RMS surface roughness from atomic force microscopy analysis was 1.6 nm for samples deposited at 19 J/cm^2 and 12.8 nm for films grown at 9 J/cm^2. It is well known that splashing of droplets or particles on the film surface is one of the drawbacks of the laser ablation technique; however, the microscopy images seem to indicate that under the conditions used the accumulation of particulates is not severe. In Fig. 9b the image of the cross section of a film grown at a pressure of 1×10^{-2} Torr and a fluence of 19 J/cm^2 is presented. No apparent columnar grain structure was observed as is often seen for vapor-deposited TiN films. This suggests that the deposits may grow as dense structures and due to the intense bombardment of the plasma since this increases the surface mobility of the depositing species and promotes a layer by layer growth.

The adhesion of the films onto the substrates has been tested by the simple Scotch-tape test. No peeling or cracking has been observed for the deposited films, indicative of good adhesion of the film. In fact, the energetic species present in the plasma should promote that the initial layers of the coat-

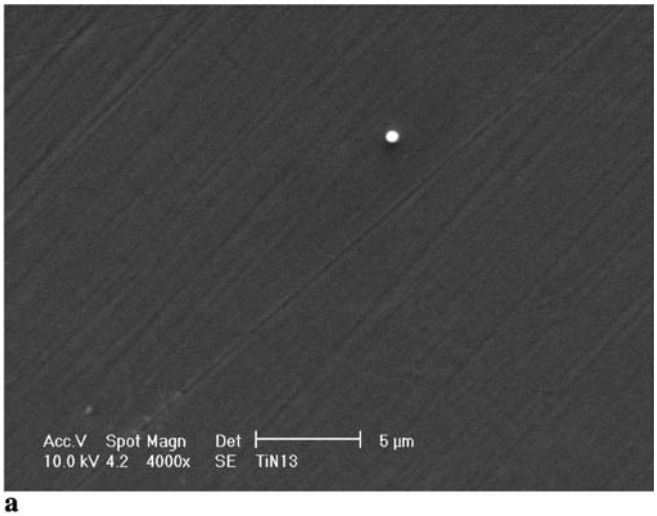

a

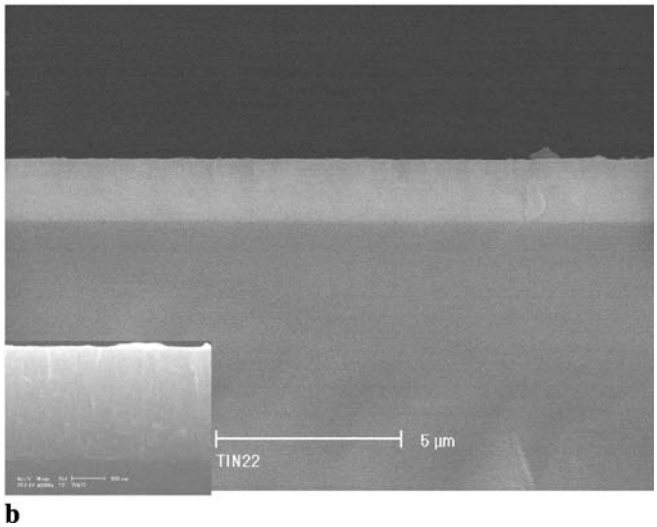

b

FIGURE 9 Scanning electron microscopy images of the deposited thin films (**a**) and image of the cross section (**b**) of a film grown at a pressure of 1×10^{-2} Torr and a fluence of 19 J/cm^2

ing be actually slightly implanted into the surface layer of the substrate forming strong metallic bonds to the substrate.

4 Conclusions

Highly textured single-phase cubic TiN films have been deposited by the laser ablation technique onto steel AISI 4140 at a substrate temperature of 230 °C and using different plasma regimes. The influence of two deposition parameters on the plasma characteristics and on the thin-film properties was investigated. An important result is that pressure controls the crystalline texture of the films. Films with a preferential orientation in the direction of the (200) plane or in the direction of the (111) plane were obtained depending on the working pressure used during deposition. Properties such as texture, hardness and grain size were characterized as a function of plasma parameters, mean ion energy and plasma density in an attempt to correlate plasma characteristics with material properties.

From the presented results it is clear that the properties of the deposited material are determined partially by a suitable combination of ion energy and plasma density, at a given pressure, and therefore these parameters might be used as control parameters in the formation of materials with specific properties.

REFERENCES

1 H.Z. Wu, T.C. Chou, A. Mishra, D.R. Anderson, J.K. Lampert, S.C. Gujrathi: Thin Solid Films **191**, 55 (1990)
2 P. Engel, G. Schwarz, G.K. Wolf: Surf. Coat. Technol. **98**, 1002 (1998)
3 N.Y. Kim, Y.B. Son, J.H. Oh, C.K. Hwangbo, M.C. Park: Surf. Coat. Technol. **128**, 156 (2000)
4 E. Valkonen, T. Karlsonn, B. Karlsonn, B.O. Johansson: Proc. SPIE Int. Tech. Conf. **401**, 41 (1983)
5 B. Zega, M. Kornmann, J. Amignet: Thin Solid Films **45**, 577 (1977)
6 M. Flores, S. Muhl, E. Andrade: Thin Solid Films **433**, 217 (2003)
7 A.J. Aronson, D. Chen, W.H. Class: Thin Solid Films **72**, 535 (1980)
8 A. Armigliato, M. Finetti, J. Garrido, S. Guerri, P. Ostoja, A. Scorzoni: J. Vac. Sci. Technol. A **3**, 2237 (1985)
9 R.S. Rawat, W.M. Chew, P. Lee, T. White, S. Lee: Surf. Coat. Technol. **173**, 276 (2003)
10 R. Chowdhury, R.D. Vispute, K. Jagannadham, J. Narayan: J. Mater. Res. **11**, 1458 (1996)
11 H.D. Gu, K.M. Leung, C.Y. Chung, X.D. Han: Surf. Coat. Technol. **110**, 153 (1998)
12 C.M. Dai, C.S. Suy, D.S. Chuu: Appl. Phys. Lett. **57**, 1879 (1990)
13 S. Metev: in *Laser Processing and Diagnostics (II)*, ed. by D. Bäuerle, K.L. Kompa, L. Laude (E-MRS Symp. Proc. **XI**) (Les Editions de Physique, Les Ulis 1986) p. 143
14 G.K. Hubler: in *Pulsed Laser Deposition of Thin Films*, ed. by D.B. Chrisey, G.K. Hubler (Wiley, New York 1994) Chapt. 13
15 S. Weissmantel, G. Reisse, D. Rost: Surf. Coat. Technol. **188–189**, 268 (2004)
16 S.S. Yap, T.Y. Tou: Appl. Surf. Sci. **248**, 340 (2005)
17 H. Riascos, G. Zambrano, P. Prieto, M. Arroyave, A. Devia, H. Galindo: Surf. Coat. Technol. **188–189**, 617 (2004)
18 T. Szorengy, E. Fogarassy, C. Fuchs, J. Hommet, L. Le Normand: Appl. Phys. A **69**, S941 (1999)
19 S. Weissmantel, G. Reisse: Diamond Relat. Mater. **10**, 1973 (2001)
20 J.M. Lackner, W. Waldhauser, R. Berghauser, R. Ebner, B. Major, T. Schöberl: Thin Solid Films **453–454**, 195 (2004)
21 A. Giardini, V. Marotta, S. Orlando, G.P. Parisi: Surf. Coat. Technol. **151–152**, 316 (2002)
22 R.K. Thareja, R.K. Dwivedi, K. Ebihara: Nucl. Instrum. Methods Phys. Res. B **192**, 301 (2002)
23 J. Herman, A.L. Thoman, C. Boulmer-Leborgne, B. Dubeuil, M.L. De Giorgi, A. Perrone, A. Luches, I.N. Mihailescu: J. Appl. Phys. **77**, 2928 (1995)
24 N.M. Bulgakova, A.V. Bulgakov, O.F. Bobrenok: Phys. Rev. E **62**, 5264 (2000)
25 W.J. Chou, G.P. Yu, J.H. Huang: Surf. Coat. Technol. **149**, 7 (2002)
26 B.D. Cullity: *Elements of X-ray Diffraction* (Ed. Pueblo y Educacion, La Habana, Cuba 1980)
27 L. Hultman, M. Shinn, P.B. Mirkarimi, S.A. Barnett: J. Cryst. Growth **135**, 309 (1994)
28 C.T. Chen, Y.C. Song, G.P. Yu, J.H. Huang: J. Mater. Eng. Perf. **7**, 324 (1998)